Polymer 55 (2014) 3573–3578

Contents lists available at ScienceDirect

Polymer

journal homepage: www.elsevier.com/locate/polymer

Diels–Alder polysulfones as dielectric materials: Computational guidance & synthesis

Robert G. Lorenzini [a, b], Jordan A. Greco [a], Robert R. Birge [a], Gregory A. Sotzing [a, b, *]

[a] Department of Chemistry, University of Connecticut, 55 North Eagleville Road, Storrs, CT 06269, United States
[b] The Polymer Program, University of Connecticut, 97 North Eagleville Road, Storrs, CT 06269, United States

ARTICLE INFO

Article history:
Received 24 April 2014
Received in revised form
11 June 2014
Accepted 13 June 2014
Available online 20 June 2014

Keywords:
Dielectric properties
Structure–property relations
Polysulfones

ABSTRACT

Herein, we describe the synthesis and characterization of polymers formed by the Diels–Alder (DA) reaction between various difurans and divinylsulfone, and evaluate their dielectric properties. These syntheses were planned with computational support *a priori* in the form of HOMO/LUMO calculations for the dienes and dienophiles, with the calculated ΔE for the DA reactions ranging between 9.33 and 9.42 eV. We describe the structure–property relationship observed when changing an atom in the linking unit between two furan rings (–CH2–, –O-, –S-, –NH–) with respect to the dielectric constant and loss tangent. Dielectric constants for the polymers range between 4.96 and 5.98, with dielectric loss tangents ranging from 0.4 to 0.9% at 1 kHz and room temperature. Bandgaps of the polymers are elucidated with UV/Visible spectroscopy, and range from 2.15 to 2.61 eV. The retro DA onset is determined using three analytical methods: thermogravimetric analysis, dynamic scanning calorimetry, and gas chromatography/mass spectrometry polymer desorption spectroscopy, and is determined to be over 125 °C in all cases.

1. Introduction

The need for high energy density capacitors is driven by their importance in various cutting-edge technologies such as medical equipment [1], electromagnetic weaponry [2], hybrid electric cars [3], and controlled nuclear fusion [4]. The current industrial standard, biaxially-oriented polypropylene (BOPP), has a dielectric constant of ~2.2 across a broad frequency range, low dielectric loss (~1×10^{-4}) and a breakdown strength of ~700 MV/m [5]. Other efforts to achieve high energy density in dielectric materials are focused on PVDF composites [6,7], aromatic polyureas and polythioureas [8,9], hybrid organic/inorganic composites [10], and the functionalization of polypropylene [11,12], among others [13]. In line with other research in our group [14–16], we seek to increase the dielectric constant of materials by the inclusion of electronegative atoms into the polymer backbones [17]. The Diels–Alder (DA) reaction involving vinyl sulfones and sulfonates are widely known in the literature for their monofunctional adducts [18–24], but to our knowledge, no groups have used them as difunctional dienophiles for inclusion in the backbone of a DA polymer. DA reactions involving furans are a facile means to increase the number of oxygen atoms in a polymer. In addition, the DA reaction does not form any side products inherent to the mechanism, and therefore does not need post-synthesis purification. Designing a sulfone group into the backbone of other polymers is known to generate high refractive indices, and therefore a high electronic contribution to the dielectric constant [25]. The difuran-divinylsulfone system (Fig. 1) is especially attractive as the two liquid monomers can form polymer films by simply mixing them and heating in an oven at 90 °C for 24 h, obviating the need for complex film processing methods. This work evaluates the potential of these polymers to serve as high dielectric constant, high bandgap dielectric materials. Elucidating the HOMO/LUMO gap between the dienes and dienophiles using commercially available computational software screens the feasibility of our syntheses before we begin work in the laboratory. We test the dielectric properties of the synthesized polymers at multiple temperatures using a time-domain dielectric spectrometer equipped with an oven. One potential difficulty with polymers formed through the DA mechanism is the possibility of the reverse, or the retro Diels–Alder (rDA) reaction. This temperature is of crucial significance, as it is the absolute maximum

* Corresponding author. Department of Chemistry, University of Connecticut, 55 North Eagleville Road, Storrs, CT 06269, United States.
E-mail address: g.sotzing@uconn.edu (G.A. Sotzing).

http://dx.doi.org/10.1016/j.polymer.2014.06.041
0032-3861/

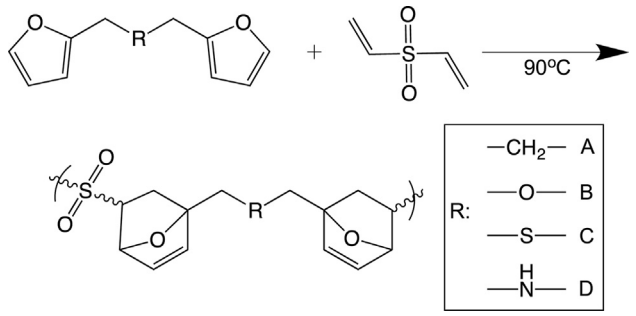

Fig. 1. Schematic of monomers and Diels–Alder polysulfones.

temperature the material could be exposed to without degradation. To probe the onset of the rDA reaction, we employ three analytical methods, each relying on different principles.

2. Experimental

2.1. Theoretical methods

All ground state geometries of divinylsulfone and the various difurans were obtained using a Becke, 3-parameter, Lee-Yang-Parr (B3LYP) hybrid functional [26] and a 6-311++G(d,2p) basis set [27,28]. Following the geometry optimizations, the self-consistent field (SCF) theory was implemented by using the restricted Hartree–Fock (RHF) [29] procedures and a 6-311++G(d,2p) basis set in order to assign the energies of the highest occupied molecular orbital (HOMO) and the lowest unoccupied molecular orbital (LUMO) for each molecule. All calculations were implemented in Gaussian 09 [30].

2.2. Monomer synthesis

1,3-Bis(2-furyl)propane (difuran **A**) was synthesized according to the literature [31] by deprotonating two equivalents of furan with n-butyllithium, followed by the addition of one equivalent of dibromopropane and vacuum distillation from the mono-substituted side product, isolated yield: 42%. ^{1}H NMR: 7.33 (2H, s), 6.31 (2H, m), 6.04 (2H, m), 2.70 (4H, t) 2.02 (2H, m).

The syntheses and ^{1}H NMR characterization of difuran monomers **B**–**D** were described in a previous publication by this group [15].

Divinylsulfone was purchased from Sigma–Aldrich and was used as received.

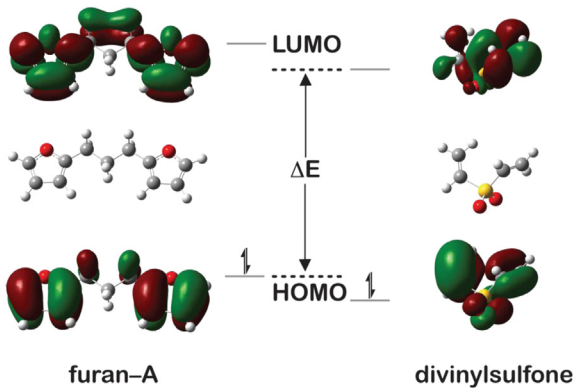

Fig. 2. Normal electron demand Diels–Alder reaction between difurans and divinylsulfone.

Table 1
Monomer HOMO, LUMO, and ΔE values.

Molecule	E_{HOMO} (eV)	E_{LUMO} (eV)	ΔE (eV)
Divinylsulfone	−11.3344	0.8289	N/A
Difuran A	−8.5177	1.0093	9.3466
Difuran B	−8.5928	1.0441	9.4217
Difuran C	−8.4970	0.9962	9.3259
Difuran D	−8.5408	1.0305	9.3697

2.3. Polymer synthesis

Equimolar amounts of divinylsulfone and a difuran were combined in a 20 mL scintillation vial and were stirred by aspirating the liquids in and out of a pipette copiously. The mixed monomers were cast onto a stainless steel shim stock sitting in an oven, and were covered with a petri dish. The oven was set at 90 °C and the reaction was allowed to proceed for 24 h.

2.4. Thermal characterization, rDA

Thermogravimetric analysis (TGA) was conducted in oxygen using a TA Instruments TGA Q500, heating rate = 10 °C/min. Differential scanning calorimetry (DSC) was conducted in nitrogen using a TA Instruments DSC Q100, heating rate = 10 °C/min. The samples were first heated to 100 °C to clear the thermal history, then were cooled to −25 °C. The presented data were obtained on the second scan. These two techniques provide information regarding the rDA temperature. Using TGA, the temperature at 2% weight loss verified the rDA as volatile monomers evaporate away. With DSC, the onset of the rDA (in the form of the onset of the simultaneous rDA and *endo–exo* isomerization) manifests itself as a broad exothermic peak. This exothermic peak persists if a second heating run is conducted, albeit shifted to a higher temperature, as the rDA remains but the endo–exo isomerization has already occurred [32].

2.5. Polymer desorption gas chromatography/mass spectrometry

The rDA was explored in a third way using a polymer desorption GC/MS method previously reported by our group [14,15]. Briefly, a 1 mg sample of polymer is added to a small glass test tube, after which it is placed in a custom-made device. The tube was dropped into the heating block of the GC/MS and desorbed materials

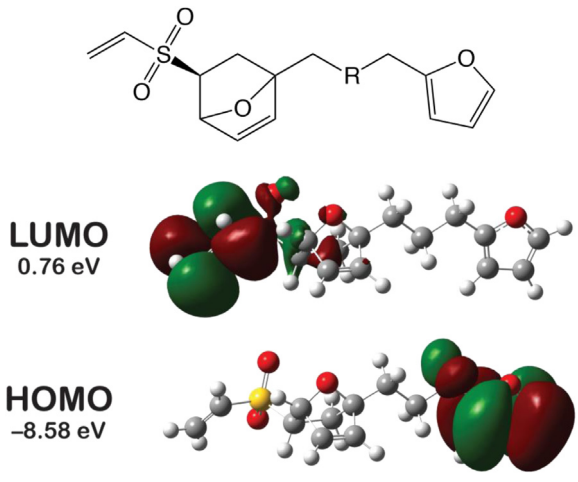

Fig. 3. Dimeric HOMO and LUMO as a model for polymerization.

Table 2
Dimeric HOMO, LUMO, and ΔE values.

Molecule	E_{HOMO} (eV)	E_{LUMO} (eV)	ΔE (eV)
Difuran A	−8.5874	0.7622	9.3496
Difuran B	−8.6837	0.7826	9.4663
Difuran C	−8.7710	0.8057	9.5768
Difuran D	−8.6315	0.7614	9.3928

proceed into the traditional GC/MS architecture. Experiments were conducted between 100 and 170 °C in 10 °C intervals.

2.6. Gel permeation chromatography

Gel permeation chromatography was done using a Waters 515 HPLC pump, Waters 2414 refractive index detector, and two mixed bed Jordi Gel DVB columns. The polymer samples were dissolved in dimethylacetamide, and the results were quantitated with polystyrene standards.

2.7. Time-domain dielectric spectroscopy

Time-domain dielectric spectroscopy was performed at the UConn Electrical Insulation Research Center using silicone-guarded rubber electrodes. Dielectric spectra and loss tangent measurements were taken at room temperature, 50, 75 and 100 °C between 10 Hz and 10 kHz.

2.8. UV/Vis spectroscopy, nuclear magnetic resonance spectroscopy

UV/Visible spectroscopy was conducted on a Varian Cary 5000 between 200 and 800 nm. Samples were prepared as follows: polymers were dissolved in chloroform, cast onto quartz slides, and dried in a vacuum oven at 50 °C for 2 h. ^{1}H NMR spectroscopy was conducted on a Bruker DMX-500, and all chemical shifts are relative to the solvent residual peak of $CDCl_3$ (δ=7.26 ppm).

3. Results & discussion

3.1. Computational HOMO/LUMO values

We theoretically examined the validity of the proposed DA polymerization reactions by carrying out a series of molecular orbital (MO) calculations with three goals. First, the favorability of the reaction is examined by calculating the properties of the relevant HOMOs and LUMOs of divinylsulfone and the difuran starting materials. Second, the MOs are examined to determine the extent to which the reactions obey Woodward–Hoffmann selection rules of the [4 + 2] cycloaddition. Finally, the relative favorability of the four different difuran starting materials is investigated.

Fig. 2 demonstrates the circumstance in which a normal electron demand mechanism is used to describe the DA polymerization mechanism. This case involves the HOMO of the diene overlapping with the LUMO of the dienophile in order to cyclize, and the bandgap (ΔE) is typically on the order of 0–12 eV. Table 1 lists the calculated energies of the frontier MOs for the monomers. The calculated ΔE values for the four difurans with divinylsulfone range between 9.33 and 9.42 eV, which is below a restrictive energy gap for the reaction. For comparison, ΔE for the well-known DA reaction between butadiene and ethylene is 10.6 eV [33]. The ΔE values for the normal electron demand mechanism (Table 1) are all lower than the respective inverse electron demand values (data not shown), in which the HOMO of the dieneophile overlaps with the LUMO of the diene. Therefore, the normal electron demand scheme will be the only one considered here. The relative ΔE values calculated for the four difuran monomers correspond to the following trend: **B** > **D** > **A** > **C**. These data suggest that greater

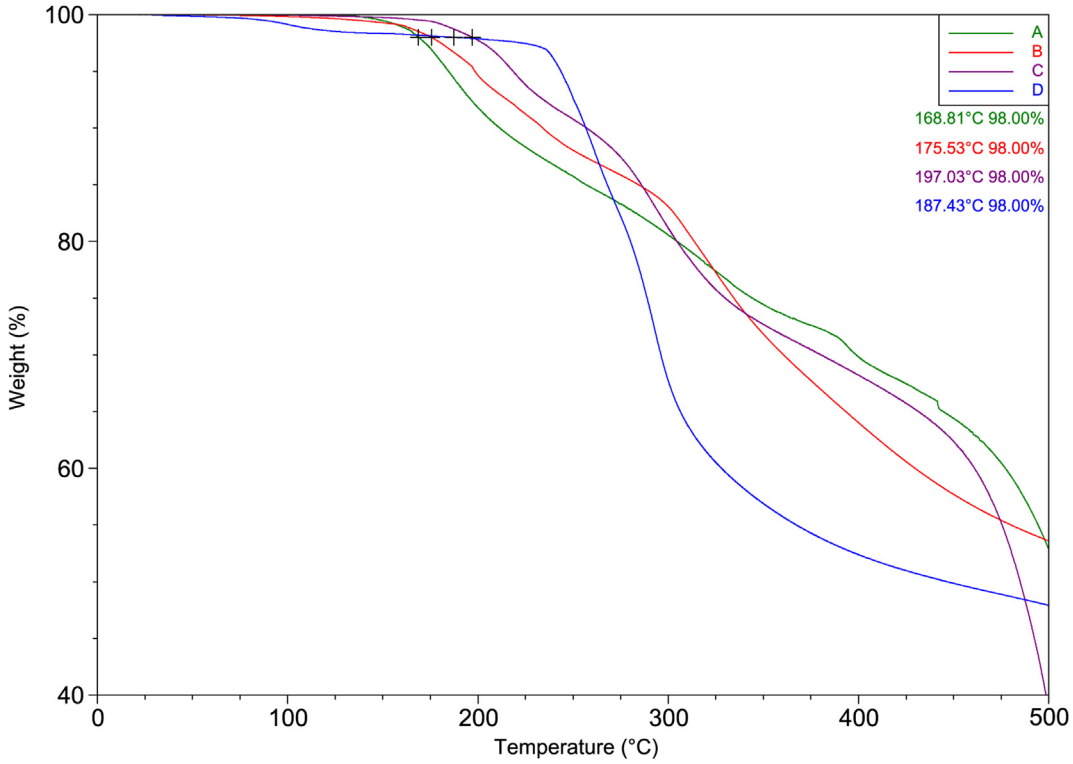

Fig. 4. TGA traces of the synthesized polymers with the 2% weight loss points highlighted.

electronegativity at the *R* position of the difurans removes electron density from the HOMO, thereby decreasing the HOMO energy and increasing ΔE.

Fig. 2 also provides an illustrative example of the frontier MOs for difuran **A** and divinylsulfone, as predicted by the calculations. The orbitals suggest Woodward–Hoffmann selection rules for a [4 + 2] cycloaddition, wherein the MO phases of the bonding π electrons are localized over the double bonds of the furan and are capable of overlapping with the virtual MO localized on the vinyl groups of divinylsulfone. Although difuran **A** is the only difuran molecule shown, the HOMO and LUMO character is qualitatively similar to that observed in Fig. 2 yielding comparable Woodward–Hoffmann selectivity.

The monomeric example provides valuable insight into the electronic features of our starting materials. However, we also investigate the case that resembles the dimeric form; in Fig. 3, one vinyl group of divinylsulfone has undergone a DA reaction with one of the furan groups of difuran **A**. The result is a molecule with the vinylsulfone group on one end and a furan group on the other, thereby mimicking the reactivity of a higher polymer. Table 2 demonstrates that the energy gap between the HOMO and LUMO for each of the four furan/sulfone dimers is the same order of magnitude as the monomeric materials. Furthermore, the HOMO and LUMO for the difurans are predicted to localize on the furan and vinyl groups of the molecules, respectively, and adhere to similar phase character that indicates Woodward–Hoffmann guidelines for the DA reaction. In this case, difuran **C** has the highest ΔE value, which is observed due to localization of the HOMO on the sulfur atom, in addition to the furan moiety. This interaction at the *R* position is unique to difuran **C**, and the other three molecules follow the electronegativity trend suggested by the results in Table 1. Despite these small differences, the computational results predict the successful DA polymerization with all difuran monomers/divinylsulfone.

Table 3
Thermal data and rDA temperatures.

Polymer	T_g, °C	rDA by GC/MS, °C	rDA by TGA, °C	rDA by DSC, °C	Mw, g/mol	Mn, g/mol	PDI
A	95	150	169	128	38,200	9500	4.02
B	47	160	176	142	54,400	12,800	4.25
C	68	170	197	143	47,000	12,600	3.73
D	113	160	187	179	46,300	8900	5.20

3.2. Thermal data, rDA, NMR

Figs. 4 and 5 show the TGA and DSC data, respectively. Table 3 shows the combined thermal data for the polymers, including the T_g and rDA temperatures elucidated through the aforementioned methods. The rDA temperatures from the three different methods are in good agreement. rDA temperatures are ubiquitously above 125 °C, and therefore will not negatively impact their potential application as dielectric materials. Of concern, however, is the fact that the T_g is observed to be within the application operating range for polymers **B** & **C**. This feature is likely responsible for the sudden increase observed in dielectric loss tangents at elevated temperatures. Because of the different DA adduct combinations during polymerization (*endo–endo*, *endo–exo*, and *exo–exo*) the NMR spectra for the polymers were difficult to quantify without synthesizing model compounds; NMR was used to confirm polymerization based on the lack of furanyl protons. Most conspicuously, the furthest upfield aromatic peaks of the furan ring present in the starting materials [15] ranging between 7.45 and 7.33 ppm were absent in the spectra obtained from the polymer samples.

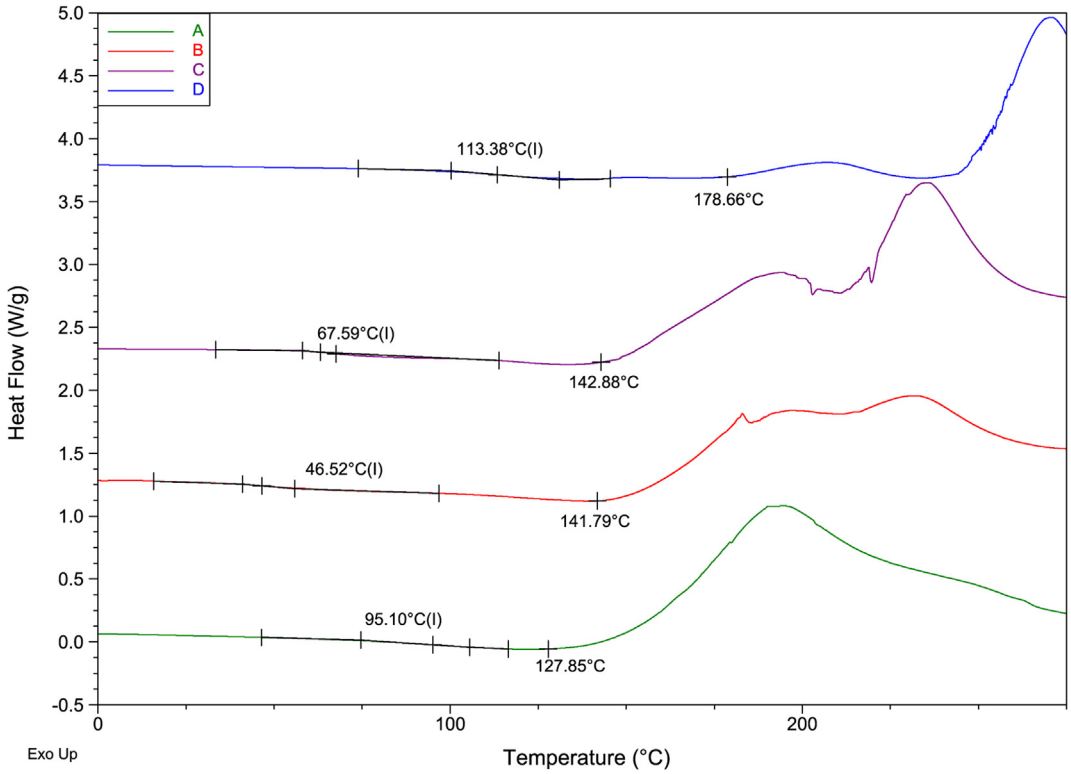

Fig. 5. DSC traces of the synthesized polymers; the *y*-axis is offset for clarity.

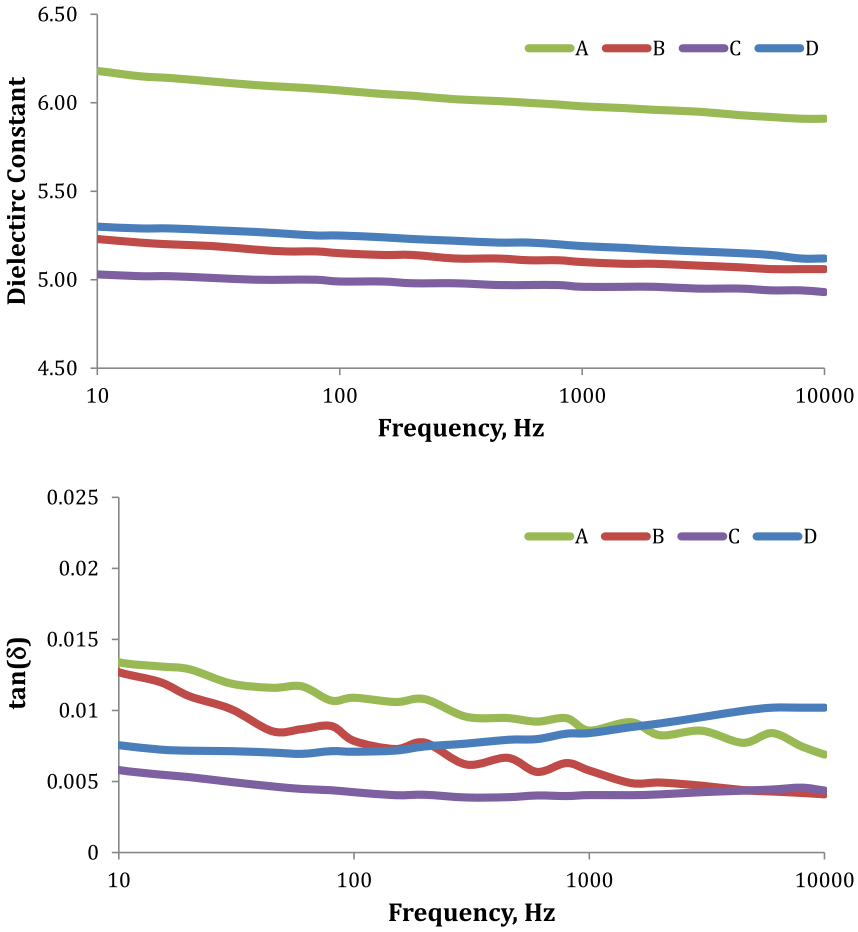

Fig. 6. Dielectric spectra (top) and dielectric loss tangents (bottom) of the synthesized polymers at room temperature.

3.3. *Dielectric spectra & trends in dielectric constant*

The dielectric spectra and loss tangents as a function of temperature are displayed in the Supporting Information, and the overlaid spectra at room temperature are shown in Fig. 6. The observed trend in dielectric constant is: **A** > **D** > **B** > **C**. We rationalize this trend by considering the local electronegativity differences between the DA adduct and the spacer units contributed by the difurans. For example, the alkyl substituent in polymer **A** makes the spacer unit have a larger difference in electronegativity overall (considering the bridging oxygen in the DA adduct) than an ether substituent, as in polymer **B**. In all cases, the dielectric constants of these polymers exceed that of BOPP (~2.2), and have dielectric loss tangents below 1.5%.

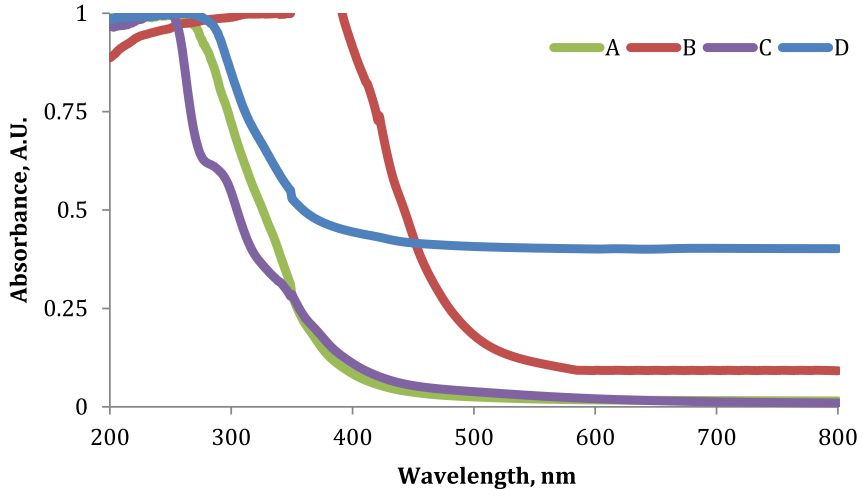

Fig. 7. UV/Vis spectra for the synthesized polymers.

Table 4
Absorbance onset wavelengths and optically determined bandgaps for the synthesized polymers.

Polymer	Absorption onset, nm	Bandgap, eV
A	520	2.39
B	579	2.15
C	555	2.24
D	477	2.61

3.4. Bandgap measurements

The UV/Vis spectra for the polymers are shown in Fig. 7. Bandgaps were calculated with the equation $E = hc/\lambda$, using the sharp absorption onset as the wavelength (Table 4). Polymer **D** was opaque to the eye, and therefore does not have an approximately zeroed baseline like the rest of the transparent polymer films. The bandgap is directly related to the maximum energy density of a dielectric material; the trend for bandgaps in these materials, in decreasing order, is **D** > **A** > **C** > **B**. This perfectly follows the electronegativity trend with respect to the central heteroatom in the difuran monomers, indicating that electron-withdrawing species increase the bandgap.

4. Conclusions

Our research group is searching for materials with high dielectric constants by exploring the chemical space synthetically, with assistance from computational and processing teams. The polymers described in this study are among others in a broad library of materials with polar groups incorporated into the polymer backbone. The dielectric data of these polymers will be fed into a quantitative structure–activity relationship (QSAR) with the hopes of finding computational descriptors that accurately predict dielectric properties. Dielectric constants for the synthesized polysulfones ranged between 4.96 and 5.98, with dielectric loss tangents ranging from 0.4 to 0.9% at 1 kHz and room temperature. Bandgaps for the polymers ranged from 2.15 to 2.61 eV. Our dielectric constants were at least double that of BOPP, the current industrial standard, which has a dielectric constant of ~2.2 across a broad frequency range. To our knowledge, this is the first time divinylsulfone has been utilized in a DA polymerization, and we intend to explore other systems using this dienophile. We believe the synergy of synthetic and computational work has the potential to move science research away from its traditionally Edisonian approach towards experiment design, which would help to save money, resources, and the environment in the process.

Acknowledgments

We would like to acknowledge Ms. JoAnne Ronzello of the UConn Electrical Insulation Research Center for conducting the dielectric measurements. We're also grateful to our funding sources, including the Office of Naval Research through the Multi-University Research Initiative (MURI) (N00014-10-1-0944) for work in the laboratory of GAS and the Harold S. Schwenk Sr. Distinguished Chair in Chemistry for work in the laboratory of RRB.

Appendix A. Supplementary data

Supplementary data related to this article can be found at http://dx.doi.org/10.1016/j.polymer.2014.06.041.

References

[1] Fazio M, Kirbie H. Ultracompact pulsed power. Proceeding of the IEEE 2004;92:1197–204.
[2] Ennis JB, MacDougall FW, Yang XH, Cooper RA, Seal K, Naruo C, et al. Recent advances in high voltage, high energy capacitor technology. In: Pulsed Power Conference, 2007 16th IEEE International, vol. 1; 2007. pp. 282–5.
[3] Tie SF, Tan CW. Renew Sustain Energy Rev 2013;20:82–102.
[4] Deshpande RP. Capicators: technology and trends tata. New Delhi: McGraw Hill Education Private Limited; 2012. p. 229.
[5] Ho J, Jow R. Characterization of high temperature polymer thin films for power conditioning capacitors. Army Res Laboratories 2009:1–28. No. ARL-TR-4880.
[6] Bhadra D, Masud MG, Sarkar S, Sannigrahi J, De SK, Chaudhuri BKJ. Polym Sci Part B Polym Phys 2012;50:572.
[7] Wang Y, Zhou X, Chen Q, Chu B, Zhang QM. IEEE Trans Dielectr Electr Insul 2010;17:1036.
[8] Wang Y, Zhou X, Lin M, Zhang QM. Appl Phys Lett 2009;94:202905.
[9] Burlingame Q, Wu S, Lin M, Zhang QM. Adv Energy Mater 2013;8:1051–5.
[10] Ha Y-G, Everaerts K, Hersam MC, Marks TJ. Acc Chem Res 2014. http://dx.doi.org/10.1021/ar4002262.
[11] Chung TCM. Green Sustain Chem 2012;2:29.
[12] Wang CC, Pilania G, Ramprasad R, Agarwal M, Misra M, Kumar S, et al. Appl Phys Lett 2013;102:152901.
[13] Ortiz RP, Facchetti A, Marks TJ. Chem Rev 2010;110:205–39.
[14] Lorenzini RG, Kline WM, Wang CC, Ramprasad R, Sotzing GA. Polymer 2013;54:3529–33.
[15] Lorenzini RG, Sotzing GA. J Appl Poly. Sci 2013. http://dx.doi.org/10.1002/APP.40179.
[16] Baldwin AF, Ma R, Wang CC, Ramprasad R, Sotzing GA. J Appl Polym Sci 2013;130:1276–80.
[17] Wang CC, Pilania G, Boggs SA, Kumar S, Breneman C, Ramprasad R. Polymer 2014. http://dx.doi.org/10.1016/j.polymer.2013.12.069.
[18] Kappe CO, Murphree SS, Padwa A. Tetrahedron 1997;42:14179–233.
[19] Fischer P, Gruner M, Jäger A, Kataeva O, Metz P. Chem Eur J 2011;17:13334–40.
[20] Fischer P, Segovia ABG, Gruner M, Metz P. Angew Chem Int Ed 2005;44:6231–4.
[21] Butt AH, Kariuki BM, Percy JM, Spencer NS. Chem Commun 2002:682–3.
[22] Zhou HB, Comninos JS, Stossi F, Katzenellenbogen BS, Katzenellenbogen JA. J Med Chem 2005;48:7261–74.
[23] Mandel J, Dubois N, Neuburger M, Blanchard N. Chem Commun 2011;47:10284–6.
[24] Carr RVC, Williams RV, Paquette LA. J Org Chem 1983;48:4976–86.
[25] Suzuki Y, Higashihara T, Ando S, Ueda M. Macromolecules 2012;45:3402–8.
[26] Becke AD. J Phys Chem 1993;98:5648–52.
[27] Clark T, Chandrasekhar J, Spitznagel GW, Schleyer PVR. J Comput Chem 1983;4:294–301.
[28] Frisch MJ, Pople JA, Binkley JS. J Chem Phys 1984;80. 265–3269.
[29] Roothaan CCJ. Rev Mod Phys 1960;32:179–85.
[30] Frisch MJ, Trucks GW, Schlegel HB, Scuseria GE, Robb MA, Cheeseman JR, et al. Wallingford, CT: Gaussian, Inc.; 2009.
[31] Lautens M, Fillion E. J Org Chem 1997;62:4418–27.
[32] Goussé C, Gandini A. Polym Int 1999;48:723–31.
[33] Gilchrist TL, Storr RC. Organic reactions and orbital symmetry. Cambridge: Cambridge University Press; 1979. p. 94.